Reversal of Neurological Defects in a Mouse Model of Rett Syndrome

Jacky Guy, *et al.*

Science **315**, 1143 (2007);
DOI: 10.1126/science.1138389

Science (print ISSN 0036-8075; online ISSN 1095-9203) is published weekly, except the last week in December, by the American Association for the Advancement of Science, 1200 New York Avenue NW, Washington, DC 20005.

of Xa-methylated genes contains several genes shown to escape X inactivation (*18*). However, given that these genes still have an elevated Xa expression level (*18*), the overall correlation between gene-body methylation and expression potentiality is maintained.

Male-to-female comparisons showed a more complete methylation level on the male X (Fig. 3A and fig. S8). Furthermore, the sites that are gene-body Xa-methylated in females are among the most highly methylated sites in males, highlighted even on the almost-complete methylation background of the male X chromosome (fig. S9).

An Xa-specific methylation present in somatic cells could reflect either methylation occurring only on Xa or demethylation occurring on Xi. The human embryonic stem (ES) cell line hES-H7 represents a stage of development just before X inactivation (*19*) and has been shown to stably maintain the appropriate characteristic methylation pattern for this stage, including allele-specific methylation (*20*). At this stage of development, the genome has presumably already undergone global demethylation and the wave of de novo methylation (*2*, *21*). Hence, we analyzed these cells using the 500K array. Out of the 116 amplicons shown to be gene-body Xa methylated, 50 also have a heterozygous genotype in H7 cells. We found that all 50 are biallelically methylated. When examining all 154 amplicons informative both for H7 and for 13130 clones, we observed that only five are monoallelically methylated in H7 cells, whereas the expected one-third are monoallelically methylated in the somatic clones (Fig. 3B). Bisulfite sequencing further verified biallelic methylation (fig. S10). Thus, given that biallelic methylation is the beginning state, demethylation of the Xi must account for the Xa-specific monoallelic pattern observed in somatic cells.

A simple model may explain both the Xa versus Xi and the gene versus intergenic differential methylation we observed: Constantly inactive regions, such as gene-poor regions and the entire Xi, may be more prone to loss of methylation maintenance (even if originally highly methylated). The resulting methylation decrease, for the entire Xi and for Xa intergenic regions, would thus highlight Xa gene body–specific methylation. At the same time, promoter CpG islands, which are protected from methylation on Xa, would remain more methylated on Xi.

In contrast to the widely held view that X chromosome allele–specific methylation is restricted to CpG islands on the inactive X, our global allele-specific methylation analyses uncovered extensive methylation specifically affecting transcribable regions (gene bodies) on the active X whether it is in the male or the female. One aspect of sex chromosome dosage compensation is the requirement for a chromosome-wide, likely epigenetic mechanism with the ability to double X-linked gene expression when necessary (i.e., in somatic cells but not in haploid germline cells). Indeed, such a phenomenon was recently described in mammals (*22*). Our finding of global elevation of methylation levels at gene bodies of both male and female active X chromosomes hints at such a chromosome-wide epigenetic control. Another example of a possible role for methylation in (potentially) active chromatin regions recently came from plants, in which extensive specific methylation of gene bodies was discovered (*23*). These results, together with the findings introduced here, should prompt reevaluation of the role of global DNA methylation that occurs away from gene promoters as well as the apparently complex relationship with chromatin activity.

Note added in proof. A second manuscript reporting gene body methylation in plants was recently published (*29*).

References and Notes

1. A. Bird, *Genes Dev.* **16**, 6 (2002).
2. T. Hashimshony, J. Zhang, I. Keshet, M. Bustin, H. Cedar, *Nat. Genet.* **34**, 187 (2003).
3. T. Mohandas, R. S. Sparkes, L. J. Shapiro, *Science* **211**, 393 (1981).
4. S. L. Gilbert, P. A. Sharp, *Proc. Natl. Acad. Sci. U.S.A.* **96**, 13825 (1999).
5. E. Heard, *Curr. Opin. Cell Biol.* **16**, 247 (2004).
6. L. F. Lock, D. W. Melton, C. T. Caskey, G. R. Martin, *Mol. Cell. Biol.* **6**, 914 (1986).
7. L. F. Lock, N. Takagi, G. R. Martin, *Cell* **48**, 39 (1987).
8. S. F. Wolf, D. J. Jolly, K. D. Lunnen, T. Friedmann, B. R. Migeon, *Proc. Natl. Acad. Sci. U.S.A.* **81**, 2806 (1984).
9. P. H. Yen, P. Patel, A. C. Chinault, T. Mohandas, L. J. Shapiro, *Proc. Natl. Acad. Sci. U.S.A.* **81**, 1759 (1984).
10. E. Viegas-Pequignot, B. Dutrillaux, G. Thomas, *Proc. Natl. Acad. Sci. U.S.A.* **85**, 7657 (1988).
11. Another recent study came to a conclusion that there is hypomethylation at gene-poor regions of the X chromosome, leading to an overall hypomethylation of Xi (*24*). Their conclusions are based entirely on the assumption that the single X chromosome of males is identical to Xa in female cells. In any case, our direct allele-specific analyses reveal only a modest hypomethylation of Xi in gene-poor regions, but a strong signature of Xi hypomethylation in gene bodies.
12. Details about the Affymetrix 500K SNP mapping array are available online (www.affymetrix.com).
13. A number of medium- to high-throughput assays have been described to analyze DNA methylation (*15*, *23*–*28*). Our methodology is most similar to the assay that used the 10K array (*28*).
14. The cocktail includes Aci I, BsaH I, Hha I, Hpa II, and HpyCH4 IV.
15. A. Schumacher *et al.*, *Nucleic Acids Res.* **34**, 528 (2006).
16. R. C. Allen, H. Y. Zoghbi, A. B. Moseley, H. M. Rosenblatt, J. W. Belmont, *Am. J. Hum. Genet.* **51**, 1229 (1992).
17. Materials and methods are available as supporting material on *Science* Online.
18. L. Carrel, H. F. Willard, *Nature* **434**, 400 (2005).
19. L. M. Hoffman *et al.*, *Stem Cells* **23**, 1468 (2005).
20. P. J. Rugg-Gunn, A. C. Ferguson-Smith, R. A. Pedersen, *Nat. Genet.* **37**, 585 (2005).
21. D. Frank *et al.*, *Nature* **351**, 239 (1991).
22. D. K. Nguyen, C. M. Disteche, *Nat. Genet.* **38**, 47 (2006).
23. X. Zhang *et al.*, *Cell* **126**, 1189 (2006).
24. M. Weber *et al.*, *Nat. Genet.* **37**, 853 (2005).
25. M. Bibikova *et al.*, *Genome Res.* **16**, 383 (2006).
26. I. Keshet *et al.*, *Nat. Genet.* **38**, 149 (2006).
27. C. M. Valley, H. F. Willard, *Curr. Opin. Genet. Dev.* **16**, 240 (2006).
28. E. Yuan *et al.*, *Cancer Res.* **66**, 3443 (2006).
29. D. Zilberman, M. Gehring, R. K. Tran, T. Ballinger, J. Henikoff, *Nat. Genet.* **39**, 61 (2007).

30. We thank H. Cedar, D. Housman, and J. Lee for discussions and comments and the staff of Harvard Medical School–Partners Healthcare Center for Genetics and Genomics Microarray Facility for Affymetrix array experiments. Support came from the NIH (to A.C.).

Supporting Online Material

www.sciencemag.org/cgi/content/full/315/5815/1141/DC1
Materials and Methods
SOM Text
Figs. S1 to S10
Tables S1 to S9

16 October 2006; accepted 22 January 2007
10.1126/science.1136352

Reversal of Neurological Defects in a Mouse Model of Rett Syndrome

Jacky Guy,[1] Jian Gan,[2] Jim Selfridge,[1] Stuart Cobb,[2] Adrian Bird[1]*

Rett syndrome is an autism spectrum disorder caused by mosaic expression of mutant copies of the X-linked *MECP2* gene in neurons. However, neurons do not die, which suggests that this is not a neurodegenerative disorder. An important question for future therapeutic approaches to this and related disorders concerns phenotypic reversibility. Can viable but defective neurons be repaired, or is the damage done during development without normal MeCP2 irrevocable? Using a mouse model, we demonstrate robust phenotypic reversal, as activation of MeCP2 expression leads to striking loss of advanced neurological symptoms in both immature and mature adult animals.

Mutations in the X-linked *MECP2* gene are the primary cause of Rett syndrome (RTT), a severe autism spectrum disorder with delayed onset that affects 1 in 10,000 girls (*1*). *MECP2* mutations are also found in patients with other neurological conditions, including learning disability, neonatal encephalopathy, autism, and X-linked mental

retardation (*2*). RTT patients show abnormal neuronal morphology, but not neuronal death (*3*), which implies that it is a neurodevelopmental rather than a neurodegenerative disorder. MeCP2 is expressed widely, but is most abundant in neurons of the mature nervous system (*4*). Conditional deletion and neuron-specific expression of *Mecp2* in mice showed that the mutant phenotype is specifically due to absence of MeCP2 in neurons (*5*–*7*). The persistent viability of mutant neurons in RTT patients raises the possibility that reexpression of MeCP2 might restore full function and, thereby, reverse RTT. Alternatively, MeCP2 may be essential for neuronal development during a specific time window, after which damage caused by its absence is irreversible. To distinguish these possibilities, we created a mouse in which the endogenous *Mecp2* gene is silenced by insertion of a *lox-Stop* cassette (*8*), but can be conditionally activated under the control of its own promoter and regulatory elements by cassette deletion (*9*) (fig. S1). Western blots (Fig. 1A) and in situ immunofluorescence (Fig. 1B) confirmed absence of detectable MeCP2 protein in *Mecp2*$^{lox\text{-}Stop/y}$ (*Stop/y*) animals. Like *Mecp2*-null mice (*6*), *Stop/y* males developed symptoms at ~6 weeks and survived for 11 weeks, on average, from birth (Fig. 1C). We concluded that the *Mecp2*$^{lox\text{-}Stop}$ allele behaves as a null mutation.

To control the activation of *Mecp2*, we combined a transgene expressing a fusion between Cre recombinase and a modified estrogen receptor (*cre-ER*) with the *Mecp2*$^{lox\text{-}Stop}$ allele (*10*). The Cre-ER protein remains in the cytoplasm unless exposed to the estrogen analog tamoxifen (TM), which causes it to translocate to the nucleus. To verify that the Cre-ER molecule did not spuriously enter the nucleus in the absence of TM and cause unscheduled deletion of the *lox-Stop* cassette, we looked for signs of *lox-Stop* deletion in *Mecp2*$^{lox\text{-}Stop/+}$,*cre-ER* (*Stop/+,cre*) females by Southern blotting. Even after 10 months in the presence of cytoplasmic Cre-ER, there was no sign of the deleted allele (Fig. 1D). The absence of spontaneous deletion of the *lox-Stop* cassette was independently confirmed by the finding that *Stop/y* males showed identical survival profiles in the presence or absence of Cre-ER (Fig. 1C). Therefore, in the absence of TM, the Cre-ER molecule does not cause detectable deletion of the *lox-Stop* cassette.

We next tested the ability of TM to delete the *lox-Stop* cassette in *Mecp2*$^{lox\text{-}Stop/y}$,*cre-ER* (*Stop/y,cre*) male mice. Five daily injections 3 to 4 weeks after birth caused 75 to 81% deletion of the cassette in brain (Fig. 1E, lanes 3, 4, and 6) and led to reexpression of the *Mecp2* gene as measured by Western blotting (Fig. 1A, lanes 4 and 5) and MeCP2 immunostaining of neurons (Fig. 1B). Activation of *Mecp2* in *Stop/y,cre* males at this stage [(Fig. 2A), bracket TM-1], before symptom onset, revealed toxicity associated with abrupt *Mecp2* reactivation, as 9 out of 17 mice developed neurological symptoms and died soon after the daily TM injection series (fig. S2). The remaining eight mice, however, did not develop any detectable symptoms, showed wild-type survival (fig. S2), and were able to breed. Four retained mice have survived for >15 months. Death of about half of animals was not due to intrinsic TM toxicity, because injected controls, including mice that had either the *Stop* allele or the *cre-ER* transgene (but not both), were unaffected. The toxic effects resembled those caused by overexpression of an *Mecp2* transgene in mice (*7, 11*), although the reactivated *Mecp2* gene retains its native promoter. The data indicate that sudden widespread activation of the *Mecp2* gene leads to either rapid death or complete phenotypic rescue.

We found that a more gradual *Mecp2* activation induced by weekly TM injections followed by three daily booster treatments eliminated toxicity. Using this scheme, we asked whether *Stop/y,cre* male mice with advanced symptoms [(Fig. 2A), bracket TM-2] could be rescued by restoration of MeCP2. To monitor the specific features of the RTT-like mouse phenotype, we devised simple observational tests for inertia, gait, hind-limb clasping, tremor, irregular breathing, and poor general condition. Each symptom was scored weekly as absent, present, or severe (scores of 0, 1, and 2, respectively). Wild-type mice always scored zero (Fig. 2B), whereas *Stop/y* animals typically showed progression of aggregate symptom scores (e.g., from 3 to 10) during the last 4 weeks of life (Fig. 2, C and E). By contrast, five out of six symptomatic *Stop/y,cre* animals were rescued by TM treat-

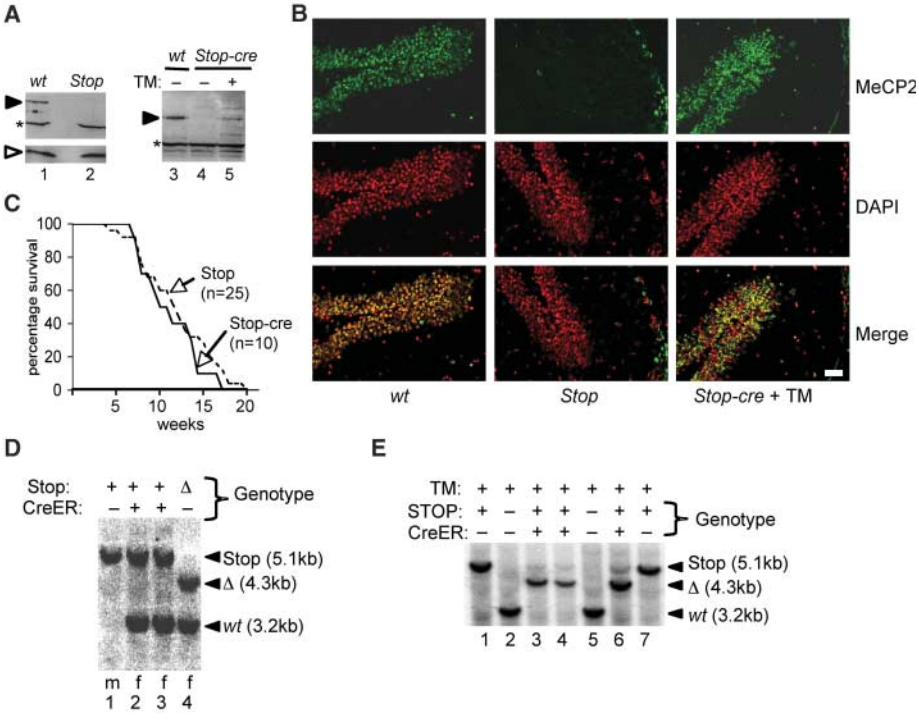

Fig. 1. Insertion of a *lox-Stop* cassette into intron 2 of the mouse *Mecp2* gene creates an allele that is effectively null, but can be activated by TM treatment. (**A**) Western blot analysis of MeCP2 protein (solid arrow) in brains of wild-type (*wt*), *Stop/y*, and *Stop/y,cre* mice before and after TM. Antibodies against MeCP2 were from J. Pevsner (left panel) and Upstate (right panel). Internal controls are nonspecific cross-reacting bands (asterisk) and bands generated by a histone H4–specific antibody (open arrow). (**B**) Detection of MeCP2 by in situ immunofluorescence in dentate gyrus of wild-type (*wt*), *Stop/y*, and TM-treated *Stop/y,cre* mice. White scale bar, 50 μm. Green cells that did not stain with DAPI (4′,6′-diamidino-2-phenylindole) in the upper *Stop* panel are nonnucleate erythrocytes showing background fluorescence. The DAPI channel was changed from blue to red using Adobe Photoshop to contrast with the green MeCP2 signal. (**C**) Comparison of the survival of *Stop/y* mice with and without the *cre-ER* transgene. (**D**) A Southern blot assay for deletion of the *lox-Stop* cassette in brains of heterozygous *Stop/+,cre* females (f) aged 10 months (lanes 2 and 3) that had not been exposed to TM. Restriction fragments from the *Mecp2 lox-Stop* (*Stop*; see male *Mecp2*$^{lox\text{-}Stop/y}$, lane 1), *Mecp2*$^{\Delta}$ with Stop deleted (Δ, see lane 4), and the wild-type (*wt*) alleles are indicated. (**E**) Southern blot assay for conversion of the *Stop* allele to the *Mecp2*$^{\Delta}$ allele (Δ) in male mouse brains after five daily TM injections. Lanes 2 and 5 show the *wt* allele.

[1]Wellcome Trust Centre for Cell Biology, Edinburgh University, The King's Buildings, Edinburgh EH9 3JR, UK. [2]Neuroscience and Biomedical Systems, Institute of Biomedical and Life Sciences, West Medical Building, University of Glasgow, Glasgow G12 8QQ, UK.

*To whom correspondence should be addressed. E-mail: a.bird@ed.ac.uk

ment. These animals initially had symptom scores of 2 or 3 and would be expected to survive for up to 4 weeks from the date of the first injection. Instead, they showed mild symptoms (see fig. S3 for examples of detailed scores) and survived well beyond the maximum-recorded life span of *Mecp2*$^{lox\text{-}Stop/y}$ animals (17 weeks) (Fig. 2, D to F, and fig. S4; see movies S1 and S2). The weekly TM injection regime, plus booster injections, gave the same level of *lox-Stop* cassette deletion as five daily TM injections (~80%) (Fig. 2G). The one animal that died had reduced *lox-Stop* cassette deletion (~50% compared with ~80%), which may explain failure to rescue.

RTT results from mosaic expression of mutant and wild-type *MECP2* alleles in the brain caused by the random inactivation of one X-linked *MECP2* allele during early female development. Heterozygous female mice may be the most appropriate model for human RTT (*12*), because both *Mecp2*$^{+/-}$ (*6*) and *Stop/+* females (Fig. 3, A, B, and E) develop RTT-like symptoms, including inertia, irregular breathing, abnormal gait, and hind-limb clasping, at 4 to 12 months of age. As in humans, the phenotype stabilizes, and the animals have an apparently normal life span. The mice often become obese, which is not a feature of the human condition. In an attempt to reverse the neurological phenotype in mature female heterozygotes, we TM-treated *Stop/+,cre* females with clear neurological symptoms. These mice progressively reverted to a phenotype that scored at or close to wild type (Fig. 3, C to E, and fig. S5 and movie S3; see fig. S3 for examples of detailed scores), including normalized weight (Fig. 3D and fig. S6). Mouse 5, for example, had a phenotypic score close to the usual plateau level and was obese at commencement of the weekly TM injection regime, but these features were both reversed (Fig. 3D). On the other hand, *Stop/+* females lacking Cre-ER did not respond to TM. Southern blots showed levels of cassette deletion in *Stop/+,cre* females that were consistently close to 50% (Fig. 3F). As the great majority of neurons became MeCP2-positive after TM treatment (fig. S7), we suspect that recombination predominantly occurs on the active X-chromosome (see legend to fig. S7). The results demonstrate that late-onset neurological symptoms in mature adult *Stop/+,cre* heterozygotes are reversible by de novo expression of MeCP2.

We also assessed the effect of *Mecp2* activation on neuronal signaling. Long-term potentiation (LTP) is reduced in the hippocampus of *Mecp2*-mutant male mice (*13*, *14*), but heterozygous females have not been tested. We performed electrophysiological analysis of *Mecp2*$^{+/-}$ heterozygous females (*6*) before and after onset of overt symptoms using both high-frequency stimulation and theta-burst (TBS) LTP induction protocols. Stimulation-response curves showed that the strength of basal synaptic transmission did not differ between symptomatic or presymptomatic *Mecp2*$^{+/-}$ female mice and wild-type littermate controls (Fig. 4A). In addition, no significant difference in hippocampal LTP between wild-type and presymptomatic females was detected. After symptom onset, however, LTP was significantly reduced in *Mecp2*$^{+/-}$ females with both protocols (Fig. 4, B and C). The magnitude of the defect was similar to that reported in *Mecp2*-null mice (*13*). To test for reversal of this effect, we measured LTP in six *Stop/+,cre* females that were TM-treated following the appearance of symptoms. LTP was measured 18 to 26 weeks after commencement of TM treatment. Control *Stop/+* and wild-type animals were also TM-treated and analyzed. The hippocampal LTP deficit was evident in symptomatic *Stop/+* mice lacking the *cre-ER* transgene, but in TM-treated *Stop/+,cre* mice, LTP was indistinguishable from wild type (Fig. 4D), which demonstrates that this pronounced electrophysiological defect is abolished in mature adults by restoration of MeCP2.

Our data show that developmental absence of MeCP2 does not irreversibly damage neurons, which suggests that RTT is not strictly a neurodevelopmental disorder. The delayed onset of behavioral and LTP phenotypes in *Mecp2*$^{+/-}$ females emphasizes the initial functional integrity of MeCP2-deficient neurons and fits with the proposal that MeCP2 is required to stabilize and maintain the mature neuronal state (*4, 6*). Consistent with the maintenance hypothesis, the time taken for major symptoms to appear postnatally in females heterozygous for an *MECP2* mutation is similar in humans (6 to 18 months) and mice (4 to 12 months), despite fundamental interspecies differences in developmental maturity at this time. The restoration of neuronal function by late expression of MeCP2 suggests that the molecular preconditions for normal MeCP2 activity are preserved in its absence. To explain this, we propose that essential MeCP2 target sites in neuronal genomes are encoded solely by patterns of DNA methylation that are established and maintained normally in cells lacking the protein. According to this hypothesis, newly synthesized MeCP2 molecules home to their correct chromosomal positions as dictated by methyl-CpG patterns and, once in place, re-

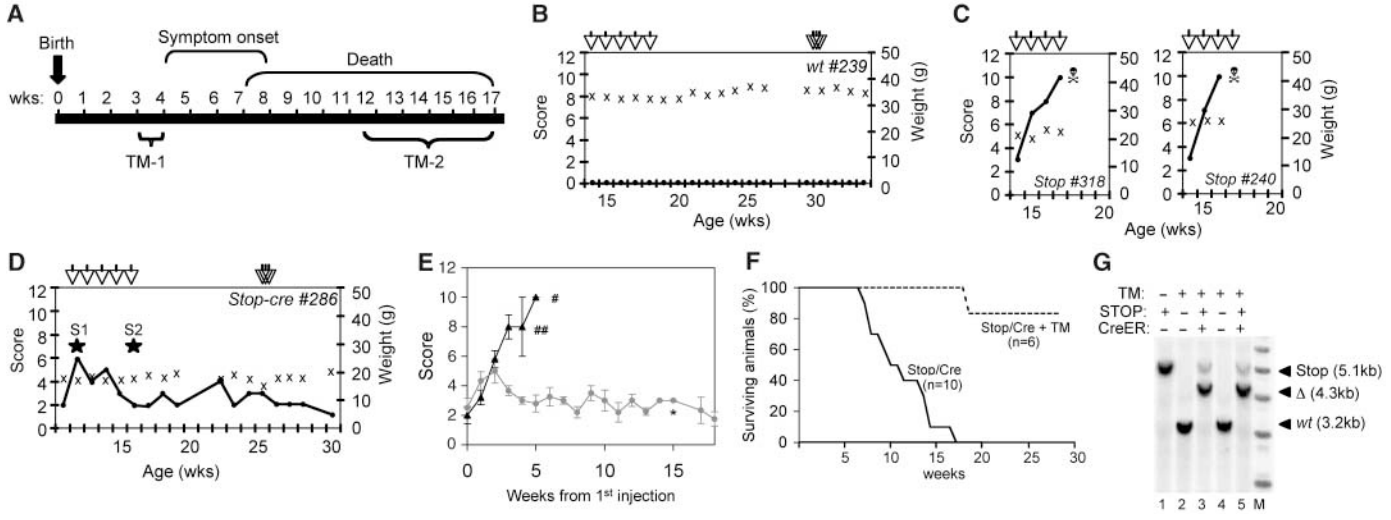

Fig. 2. Reversal of the neurological phenotype by activation of the *Mecp2* gene in *Stop/y,cre* males. (**A**) Time course of the *Stop/y* phenotype. (**B**, **C**, and **D**) Plots of the phenotypic scores (●) and weights (x) of individual wild-type (*wt*) (B), *Stop/y* (*Stop*) (C), and *Mecp2*$^{lox\text{-}Stop/y}$*,cre-ER* (*Stop-cre*) (D) animals after TM injections (vertical arrows). (See also fig. S2.) Stars in (D) indicate when the clips shown in movies S1 and S2 were recorded. (**E**) Aggregate symptom score profiles following TM injection of *Stop/y,cre* (○, n = 3 to 6, except *, which was a single animal) and *Stop/y* (▲, n = 4 to 5; except ## and #, which are 2 and 1 data points, respectively) mice. (**F**) Survival profiles of TM-treated *Stop/y,cre* mice and control *Stop/y* mice. (**G**) Southern blot showing deletion of the lox-Stop cassette (lanes 3 and 5) after a weekly TM injection regime + booster injections.

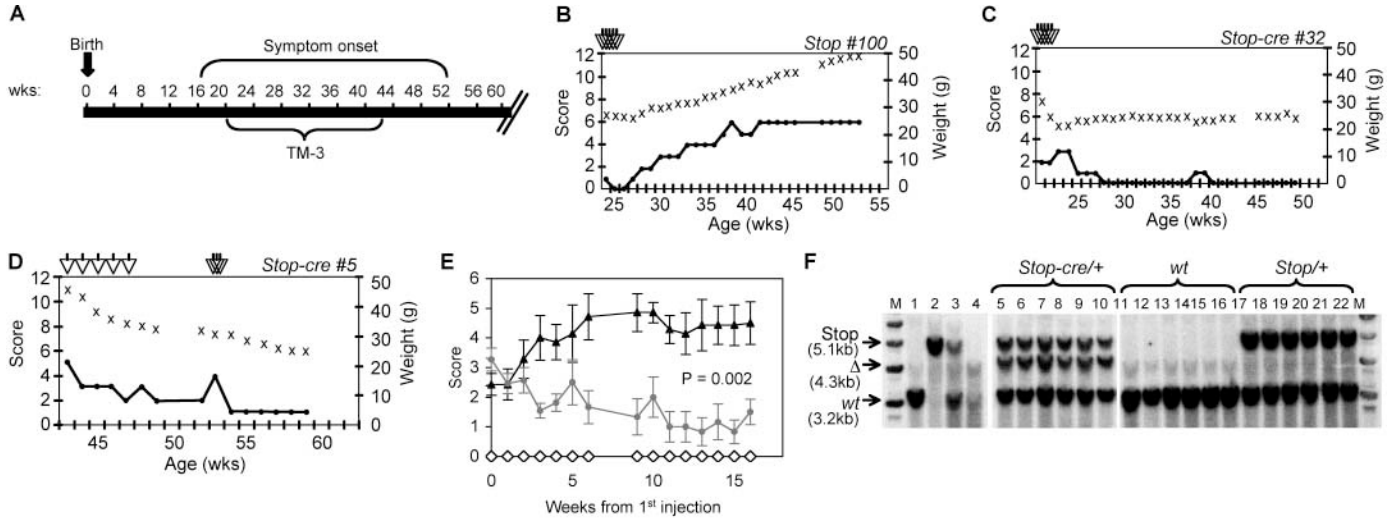

Fig. 3. Reversal of late-onset neurological symptoms by *Mecp2* gene induction in mature adult *Stop/+,cre* females. (**A**) Time course of symptom onset. TM administration began during the bracketed period (TM3). (**B**, **C**, and **D**) Phenotype (●) and weight (x) profiles for a *Stop/+* female (B) and two *Stop/+,cre* females (C and D). All animals shown were subjected to either five daily TM injections or five weekly plus three booster TM injections (vertical arrows). Animals subject to weekly injection regimes were scored blind as part of a mixed genotype cohort. (**E**) Plot of average symptom scores for females with *wt* (◇, n = 5 to 6), *Stop/+* (▲, n = 6 to 7), and *Stop,+,cre* (●, n = 5 to 11) genotypes. Repeated measures analysis of variance (ANOVA) compared *Stop/+* and *Stop/+,cre* female scores in weeks 11 to 16. (**F**) Southern blot analysis of the effects of TM treatment on a cohort including six *Stop/+,cre* (lanes 5 to 10), six *wt* (lanes 11 to 16) and six *Stop/+* (lanes 17 to 22) females. All three genotypes received TM. Restriction fragments derived from *Mecp2 lox-Stop* (Stop), deleted $Mecp2^{\Delta}$ (Δ) and wild type (*wt*) are marked with arrows. Brain DNA from animals 32 and 5 shown above are in lanes 9 and 6, respectively. Lanes 1 to 4 show blots of *wt* male, *Stop/y* male, *Stop/+* female, and $Mecp2^{\Delta/+}$ female, respectively.

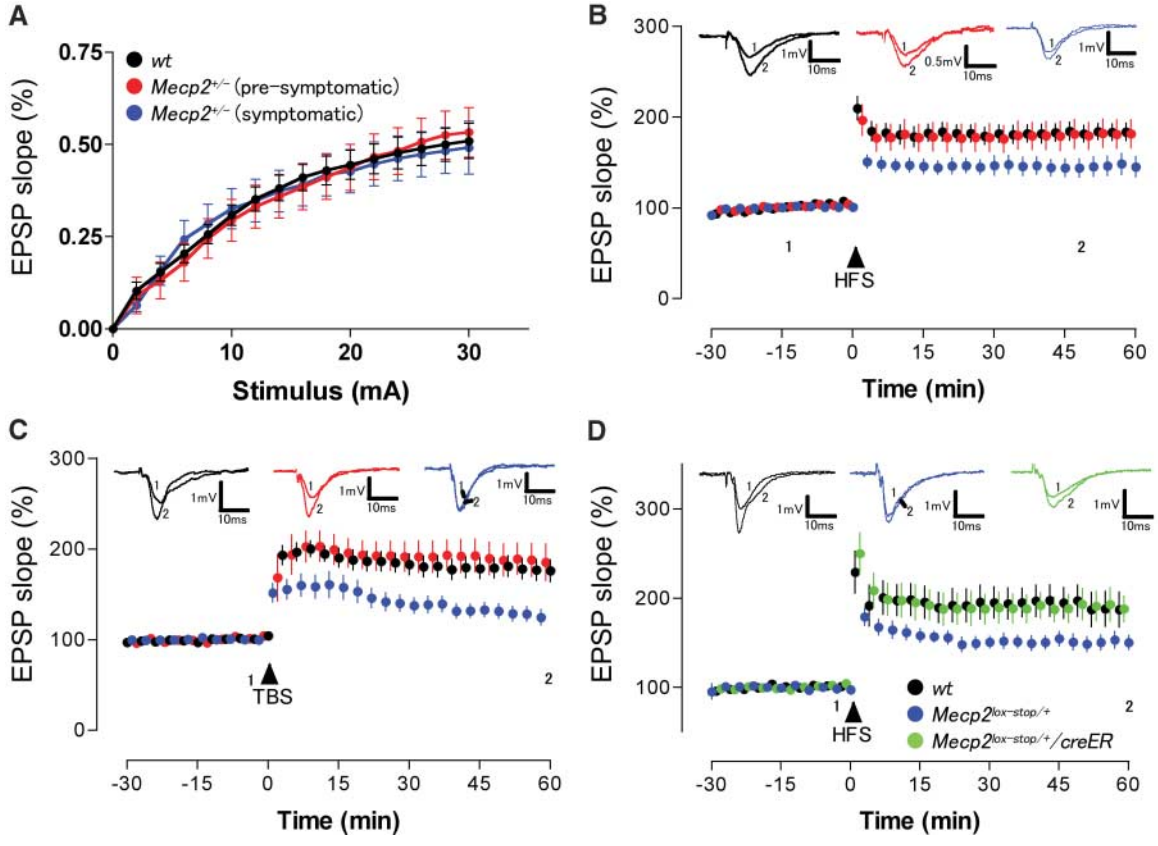

Fig. 4. A deficit in long-term potentiation (LTP) accompanies onset of symptoms in mature adult $Mecp2^{lox\text{-}Stop/+}$ heterozygous females and is reversed by *Mecp2* reactivation. (**A**) Stimulation-response curves in symptomatic (blue) or presymptomatic (red) $Mecp2^{+/-}$ female mice and *wt* littermate controls (black; all $P > 0.05$). (**B**) Measurements of LTP using a high-frequency stimulation (HFS) paradigm in presymptomatic (n = 9; $P > 0.05$), symptomatic (n = 9; $P < 0.05$) $Mecp2^{+/-}$ mice, and *wt* female littermate control groups (n = 7 and 8; pooled data plotted). (**C**) Measurements of LTP using theta-burst stimulation in presymptomatic (n = 9; $P > 0.05$), symptomatic (n = 9; $P < 0.05$) $Mecp2^{+/-}$ mice, and *wt* female littermate control groups (n = 7 and 8). (**D**) HFS-induced LTP measurements in TM-treated symptomatic *Stop/+* mice (n = 11; $P < 0.05$), *Stop/+,cre* mice (n = 10; $P > 0.05$), and *wt* mice (n = 9; $P > 0.05$). Recombination data are shown in Fig. 3F. Insets in (B) to (D) show representative voltage traces before (1) and after (2) LTP induction. Two-way repeated measures ANOVA was used to assess significance throughout.

sume their canonical role as interpreters of the DNA methylation signal (*15, 16*).

Our study shows that RTT-like neurological defects due to absence of the mouse *Mecp2* gene can be rectified by delayed restoration of that gene. The experiments do not suggest an immediate therapeutic approach to RTT, but they establish the principle of reversibility in a mouse model and, therefore, raise the possibility that neurological defects seen in this and related human disorders are not irrevocable.

References and Notes

1. R. E. Amir *et al.*, *Nat. Genet.* **23**, 185 (1999).
2. J. L. Neul, H. Y. Zoghbi, *Neuroscientist* **10**, 118 (2004).
3. D. Armstrong, J. K. Dunn, B. Antalffy, R. Trivedi, *J. Neuropathol. Exp. Neurol.* **54**, 195 (1995).
4. N. Kishi, J. D. Macklis, *Mol. Cell. Neurosci.* **27**, 306 (2004).
5. R. Z. Chen, S. Akbarian, M. Tudor, R. Jaenisch, *Nat. Genet.* **27**, 327 (2001).
6. J. Guy, B. Hendrich, M. Holmes, J. E. Martin, A. Bird, *Nat. Genet.* **27**, 322 (2001).
7. S. Luikenhuis, E. Giacometti, C. F. Beard, R. Jaenisch, *Proc. Natl. Acad. Sci. U.S.A.* **101**, 6033 (2004).
8. I. Dragatsis, S. Zeitlin, *Nucleic Acids Res.* **29**, E10 (2001).
9. Materials and Methods are available as supporting material on *Science* Online.
10. S. Hayashi, A. P. McMahon, *Dev. Biol.* **244**, 305 (2002).
11. A. L. Collins *et al.*, *Hum. Mol. Genet.* **13**, 2679 (2004).
12. S. Kriaucionis, A. Bird, *Hum. Mol. Genet.* **12** (spec. issue 2), R221 (2003).
13. Y. Asaka, D. G. Jugloff, L. Zhang, J. H. Eubanks, R. M. Fitzsimonds, *Neurobiol. Dis.* **21**, 217 (2005).
14. P. Moretti *et al.*, *J. Neurosci.* **26**, 319 (2006).
15. X. Nan, J. Campoy, A. Bird, *Cell* **88**, 471 (1997).
16. J. D. Lewis *et al.*, *Cell* **69**, 905 (1992).

17. We are grateful to A. McClure and D. DeSousa for excellent technical assistance; to S. Zeitlin and J. Pevsner for reagents; and to D. Kleinjan, I. Vida, and R. Morris for comments on the manuscript. The work was funded by the Wellcome Trust, the Rett Syndrome Research Foundation (USA), and Rett Syndrome UK/Jeans for Genes.

Supporting Online Material

www.sciencemag.org/cgi/content/full/315/5815/1143/DC1
Materials and Methods
Figs. S1 to S7
References
Movies S1 to S3

4 December 2006; accepted 18 January 2007
10.1126/science.1138389